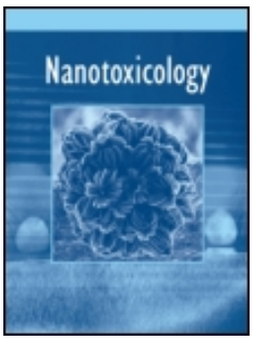

Nanotoxicology

ISSN: 1743-5390 (Print) 1743-5404 (Online) Journal homepage: http://www.tandfonline.com/loi/inan20

Persistence of silver nanoparticles in the rat lung: Influence of dose, size, and chemical composition

Donald S. Anderson, Rona M. Silva, Danielle Lee, Patricia C. Edwards, Arjun Sharmah, Ting Guo, Kent E. Pinkerton & Laura S. Van Winkle

To cite this article: Donald S. Anderson, Rona M. Silva, Danielle Lee, Patricia C. Edwards, Arjun Sharmah, Ting Guo, Kent E. Pinkerton & Laura S. Van Winkle (2015) Persistence of silver nanoparticles in the rat lung: Influence of dose, size, and chemical composition, Nanotoxicology, 9:5, 591-602, DOI: 10.3109/17435390.2014.958116

To link to this article: http://dx.doi.org/10.3109/17435390.2014.958116

http://informahealthcare.com/nan
ISSN: 1743-5390 (print), 1743-5404 (electronic)

Nanotoxicology

Nanotoxicology, 2015; 9(5): 591–602
 DOI: 10.3109/17435390.2014.958116

informa
healthcare

ORIGINAL ARTICLE

Persistence of silver nanoparticles in the rat lung: Influence of dose, size, and chemical composition

Donald S. Anderson[1], Rona M. Silva[1], Danielle Lee[1], Patricia C. Edwards[1], Arjun Sharmah[2], Ting Guo[2], Kent E. Pinkerton[1,3,4], and Laura S. Van Winkle[1,3]

[1]Center for Health and the Environment,University of California Davis, Davis, CA, USA, [2]Department of Chemistry, [3]Department of Anatomy, Physiology and Cell Biology, School of Veterinary Medicine, and [4]Department of Pediatrics, School of Medicine, University of California Davis, Davis, CA, USA

Abstract

Increasing silver nanoparticle (AgNP) use in sprays, consumer products, and medical devices has raised concerns about potential health effects. While previous studies have investigated AgNPs, most were limited to a single particle size or surface coating. In this study, we investigated the effect of size, surface coating, and dose on the persistence of silver in the lung following exposure to AgNP. Adult male rats were intratracheally instilled with four different AgNPs: 20 or 110 nm in size and coated with either citrate or polyvinylpyrrolidone (PVP) at 0.5 or 1.0 mg/kg doses. Silver retention was assessed in the lung at 1, 7, and 21 d post exposure. ICP-MS quantification demonstrated that citrate-coated AgNPs persisted in the lung to 21 d with retention greater than 90%, while PVP-coated AgNP had less than 30% retention. Localization of silver in lung tissue at 1 d post exposure demonstrated decreased silver in proximal airways exposed to 110 nm particles compared with 20 nm AgNPs. In terminal bronchioles 1 d post exposure, silver was localized to surface epithelium but was more prominent in the basement membrane at 7 d. Silver positive macrophages in bronchoalveolar lavage fluid decreased more quickly after exposure to particles coated with PVP. We conclude that PVP-coated AgNPs had less retention in the lung tissue over time and larger particles were more rapidly cleared from large airways than smaller particles. The 20 nm citrate particles showed the greatest effect, increasing lung macrophages even 21 d after exposure, and resulted in the greatest silver retention in lung tissue.

Keywords

Clearance, intratracheal instillation, macrophage, respiratory

History

Received 3 June 2014
Revised 20 August 2014
Accepted 21 August 2014
Published online 18 September 2014

Introduction

Silver nanoparticles (AgNPs) are used as anti-microbial agents in wound dressings, sprays, textiles, and medical devices (Pelgrift & Friedman, 2013). The increasing prevalence of AgNPs has led to concerns about accumulation in the environment as well as possible health effects (Fabrega et al., 2011, Seltenrich, 2013). Further, because AgNPs are small, there is concern about persistence of these materials in the body following multiple routes of exposure, including exposures to the respiratory system. Inhalation has been proposed as a route of exposure not only during the production of these materials but also during the use of sprays (Quadros & Marr, 2010).

Previous work on the distribution of AgNPs in the respiratory system has been limited to studies that examine a single nanoparticle surface coating or size. The bulk of previous studies do not describe the distribution of the particles within the lung or measure the amount of silver retained in the lungs over time. Studies that compare inhalation versus instillation of insoluble particles have shown that clearance of instilled particles is slower than that of inhaled particles (Pritchard et al., 1985) and that biological effects may be larger for instilled particles at the same delivered dose (Baisch et al., 2014). Instillation enables screening of a large number of compounds, at a range of doses, including high doses, rapidly and delivery of a readily quantifiable, known delivered dose (Driscoll et al., 2000). All these features are advantageous for the measurement of particle retention and eventual clearance from the lungs over time, especially when the sensitivity of the measurement is an issue.

One mechanism of removal of particles in the lung is uptake by inflammatory cells. As clearance of particles is dependent on both the mucociliary escalator and phagocytes for removal of particles, the use of multiple doses to characterize retention and distribution is important as these processes may be saturable. Macrophages are the predominant inflammatory phagocytic cell-type resident and recruited to the lung, often comprising 98% or more of the cells obtained in bronchoalveolar lavage. Hence, when studying long-term clearance of nanoparticles from the lung tissue, assessment of macrophage involvement is key to fully understanding the response.

Ag nanomaterials can be stabilized using surface coatings to prevent oxidation and loss of Ag ions. Citrate and polyvinylpyrrolidone (PVP) are common surface coatings used to stabilize AgNPs in solution (Huynh & Chen, 2011). Surface-absorbed PVP stabilizes AgNPs by steric repulsion (Huynh & Chen, 2011).

Correspondence: Laura Van Winkle, PhD, DABT, Department of Anatomy, Physiology and Cell Biology, School of Veterinary Medicine, University of California Davis, One Shields Ave, Davis, CA 95616, USA. Tel: +1 530 754 7547. E-mail: lsvanwinkle@ucdavis.edu

While PVP is generally considered safe by the US Food and Drug Administration, there have been documented cases of allergic reaction to PVP (Adachi et al., 2003; Rönnau et al., 2000; Yoshida et al., 2008). Previous studies of both citrate and PVP stabilized AgNPs administered *in vitro,* and in mice *in vivo,* have found that silver associated with small (20 nm) citrate-coated AgNPs were still detected in the lung tissue, associated with extracellular matrix, at 40 h and 21 d after a single instillation (Wang et al., 2014). However, the effect of varying doses on the localization of AgNPs by lung region, and within lung cells, was not described.

In the lung, the effect of materials on the respiratory tract is greatly influenced by the lung region that receives the highest deposition (local delivered dose). Retention may also be very important for AgNPs because the nature of these particles may change over time, potentially releasing silver ions (Wang et al., 2014). We used two doses and four types of AgNPs: citrate coated 20 and 110 nm AgNPs and PVP coated 20 and 110 nm AgNPs as well as site-specific histopathology to evaluate AgNP effects by the lung region. We coupled this histologic approach with quantitative analysis of total lung silver burden over time following a single acute exposure. The goal was to determine: (1) how size and surface coating influence silver retention in the lung; (2) where in the lung the silver was retained and whether that changed over time; and (3) the extent of macrophage involvement in the silver clearance over time. These data will inform future studies of health effects of AgNPs health effects in the lung because biological effects within the lung tissue can be discussed in terms of clearance and retention of the initial dose.

Methods

Silver nanoparticles

AgNPs manufactured by nanoComposix, Inc (San Diego, CA) were supplied by the National Institute of Environmental Health Sciences Centers for Nanotechnology Health Implications Research (NCNHIR) consortium. Preliminary testing and characterization of the materials were performed by The Nanotechnology Characterization Laboratory (SAIC-Frederick, Frederick, MD) (Wang et al., 2014). Two sizes, 20 nm and 110 nm, were used and were stabilized in two different buffers, citrate and polyvinylpyrrolidone (PVP), to yield four test particles that were delivered intratracheally (i.t.) as 0.5 and 1.0 mg/kg. Doses were chosen to match those used in the previous studies performed by NCNHIR consortium members to allow comparison across studies (Wang et al., 2014). Two PVP buffers were used as controls for the PVP-coated particles: 10 kDa PVP (ISP Technologies Inc., Texas City, TX) for the 20 nm Ag NPs and 40 kDA PVP (Calbiochem, San Diego, CA) for the 110 nm AgNPs. Sham controls included the use of endotoxin-free water with the coating material at a similar concentration to that in the AgNP suspensions so that the effects of the coating could be separated from AgNP effects. The PVP was used at 33 μg/ml for the 10 kDa PVP and 62 μg/ml for the 40 kDa PVP. Citrate buffer was prepared using trisodium citrate dihydrate (Sigma, St. Louis, MO) in endotoxin-free water to a concentration of 2 mM and pH 7.5. All AgNPs were supplied at 1 mg/ml and a dilution of 0.5 mg/ml was made by mixing the provided AgNP suspensions with the corresponding buffers. AgNP stock suspensions were sonicated in a Branson Ultrasonics 8510 bath sonicator (Danbury, CT) for 5 min immediately prior to use.

AgNP characterization

Dynamic light scattering (DLS) and transmission electron microscopy (TEM) were performed to characterize AgNPs prior to use. DLS was performed on samples diluted 1:100 in milliQ water with a Zetasizer Nanosizer ZEN1690 (Malvern Instruments, Malvern, UK) equipped with a He–Ne 633 nm laser. Diluted sample absorbance was determined using a PharmaSpec UV-1700 spectrophotometer (Shimadzu, Santa Clara, CA) and the refractive index of silver was obtained from the NIST database (Smith & Fickett, 1995). TEM sample grids were prepared by drop-coating the sample solution onto the Lacey Carbon Type-A, 300 mesh Cu grids (Ted Pella Inc, Redding, CA). Briefly, 6 μL of aqueous sample was placed on the TEM grid and allowed to dry for 2 h. Imaging was performed using Phillips CM12 Transmission Electron Microscope (Ted Pella Inc, Redding, CA) at 100 kV.

Animals

Twelve-week-old male Sprague–Dawley rats were obtained from Harlan Laboratories (Hayward, CA) and acclimated for 1 week prior to treatment. Rats were housed two per cage and provided Laboratory Rodent Diet (Purina Mills, St Louis, MO) and water *ad libitum*. All animal experiments were performed under protocols approved by the University of California Davis IACUC in accordance with National Institutes of Health guidelines. For intratracheal instillation, rats were instilled with 1 μl/g body weight of AgNP suspension or vehicle control buffer under anesthesia administered via a Quantiflex anesthesia unit (Medmark Crop., Versailles, OH). The anesthesia unit was equipped with an isoflurane vaporizer using 3% isoflurane in an oxygen flow of 1.0 l/min for 5–6 min. Biological samples were obtained at necropsy 1, 7, and 21 d post instillation following anesthesia with Beuthanasia-D at 7.5 ml/kg and exsanquination. The trachea was cannulated and the left lung lobe was isolated by clamping the left primary bronchus. The right lobes were lavaged using 8 ml of 0.9% sterile saline in a 12-ml syringe, washing with the same aliquot for three times. The resultant bronchoalveolar lavage fluid (BALF) was collected into 15 ml round bottom tubes and kept on ice until processed. The right lobes were removed and stored at −80 °C. The left lobe of most animals was perfused with 4% paraformaldehyde at 30 cm of pressure for 1 h. There were six animals per treatment at each timepoint tested ($N = 6$/group and timepoint).

BALF macrophages

BALF was centrifuged at 2000 rpm and 4 °C for 10 min to pellet cells. The supernatant was removed and the cell pellet was resuspended in 2 ml sterile 0.9% saline and the total number of cells and non-viable cells, using Trypan blue assay, was counted. Cytospin slides were prepared from the resuspended BALF cells for silver staining and quantitation of macrophages as a percentage of the total cells.

Silver staining

Two 1 mm blocks representing short- and long-axial path airways of the 4% paraformaldehyde fixed left lobe were embedded in paraffin and sectioned onto poly-L-lysine-coated slides. Silver was visualized using a variation of the published method for autometallography (Danscher et al., 2006; Hacker et al., 1988). A silver enhancement kit for light and electron microscopy (Ted Pella Inc, Redding, CA) was used (Wang et al., 2014), and all slides were developed under identical conditions to facilitate comparisons across groups and timepoints. Paraffin-embedded samples were deparafinized, rehydrated, and stained with equal volumes of enhancer and developer for 15 min. Cytospin slides were hydrated in PBS, stained for silver as described above, and then lightly counter stained with diluted 1:1000 methylene blue azure II stain.

BALF macrophage counts

The percentage of silver-positive BALF macrophages was determined in cytospins stained by autometallography and counted for silver positive and negative macrophages at 40 × magnification. A total of 500 cells were counted per slide. To further assess the silver load in the macrophage population, a semi-quantitative scoring system was employed. Silver-positive macrophages were subdivided into light, moderate, and heavy staining for silver as shown in Figure S1. Two-hundred silver positive macrophages were scored per animal; all silver positive macrophages were scored if less than 200 macrophages were silver positive. The determined fractions of light, moderate, and heavy silver content macrophages were used to determine a score for each animal using the following formula:

$S=((M_T\times f_L)+(M_T\times f_M\times 2)+(M_T\times f_H\times 3))/1000$ where S is the silver score, M_T is the total recovered macrophages per ml of BALF, and f_L, f_M, and f_H are the fractions of silver positive macrophages in the macrophage population.

TEM of BALF macrophages

Cells recovered from BALF were fixed with Karnovsky's fixative (0.9% glutaraldehyde/0.7% paraformaldehyde in cacodylate buffer, adjusted to pH 7.4, 330 mOsmol) and suspended in agar blocks. Blocks were embedded in Araldite 502 resin and osmicated (Van Winkle et al., 1995). Sections were cut using a Leica Ultracut UCT ultramicratome and Diatome diamond knives (Ted Pella Inc, Redding, CA). TEM images of BALF macrophages were obtained using a Phillips CM120 electron microscope (Ted Pella Inc, Redding, CA).

Silver deposition quantification

The concentration of silver in the right middle lobe was determined using ICP-MS on the snap frozen right middle lobe stored at −80 °C. The lobes were lyophilized using a Labconco FreeZone 2.5 (Kansas City, MO) freeze drying system and weighed to determine tissue dry weight. Tissue was digested with 70% trace metal grade nitric acid (Fisher, Pittsburg, PA) and heated to 70 °C for 2 h. Samples were cooled to room temperature, and an equal volume of 30% H_2O_2 was added. Samples were reheated to 70 °C for 2–4 h to break down remaining lipids and finally cooled to room temperature and diluted 10:1 with 3% HNO_3 for analysis by the UC Davis/Interdisciplinary Center for Plasma Mass Spectrometry using an Agilent 7500CE ICP-MS (Agilent Technologies, Palo Alto, CA) (Abid et al., 2013). The samples were introduced using a MicroMist Nebulizer (Glass Expansion, Pocasset, MA) into a temperature-controlled spray chamber with Helium as the collision cell gas. Instrument standards were diluted from Certiprep Ag Standard (SPEX CertiPrep, Metuchen, NJ) to 0.5 ppb, 1 ppb, 10 ppb, 50 ppb, 100 ppb, 200 ppb, and 500 ppb in 3% Trace Element HNO_3 (Fisher, Hudson, NH) in 18.2 MΩ cm water. A NIST 1643E Standard (National Institute of Standards and Technology, Gaithersburg, MD) was analyzed initially and QC standards consisting of a Certiprep Ag Standard at a concentration of 100 ppb was analyzed every 12th sample as a quality control. Sc, Y, and Bi Certiprep standards (SPEX CertiPrep) were diluted to 100 ppb in 3% HNO_3 and introduced by peripump as an internal standard.

Semi-quantitative scoring

The level of silver present in the terminal bronchioles of the left lung lobe was assessed using a semi-quantitative scoring system (Coppens et al., 2007). Silver-enhanced stained slides were blinded and scored on a scale of 0–4 using the criteria described in Supplemental Table 1. All terminal bronchioles in the two pathway sections were scored and the mean was taken to represent that animal. Six animals were counted per group.

Statistics

Data are reported as mean ± standard error of the mean (SEM) unless otherwise stated. Statistical outliers were eliminated using the extreme deviate method (Graphpad, La Jolla, CA). Multivariate analysis of variance (MANOVA) was applied against particle size, surface coating, time-point, and dose when appropriate. Multiple comparisons for factors containing more than two levels were performed using Fisher's Protected Least Significant Difference (PLSD) method. Pair-wise comparisons were performed individually using a one-way ANOVA followed by PLSD *post hoc* analysis. Non-parametric data analysis was performed using a Kruskal–Wallis ANOVA and Median test or a Mann–Whitney test where appropriate. p values of <0.05 were considered statistically significant. Statistics was performed using STATISTICA 64 (STATISTICA Enterprise Workstation, Tulsa, OK).

Results

Particle characterization

All AgNPs were supplied by the NIEHS NCNHIR and NCI and were previously characterized (Wang et al., 2014). TEMs of both sizes of particles (Figure S2) in suspension at the time of instillation indicate AgNP of the expected sizes. Some particle clumping in suspension is expected. DLS confirmed that sonication just prior to instillation results in single particles of the expected size. The diameter of the 110 nm citrate AgNP was 108.5 nm and the 20 nm citrate was 19.5 nm. These results are in agreement with other studies using the same particles and resuspension methods (Wang et al., 2014). It should be noted that these are measures of the core silver particle size and protein corona and surface modifications could add to this size.

Macrophage clearance of AgNP

BALF cells were tested for viability and the percentage of non-viable cells was not different between the control (a range of 1.2–2.2%) and exposed (a range of 2.3–3.5%) groups. BALF cells were stained for silver content and the predominant BALF cell type that contained silver, as determined by autometallography, was the macrophage population (Figure S1). Within this population, there were a variety of macrophage profiles with the majority of profiles containing no silver stain (Figure S1B) and the remainder containing various amounts of silver (Figure S1A–D). These profiles were similar between all four particle types. Some macrophages were loaded with silver and had a foamy appearance (Figure S1D). When total macrophage cell numbers were examined (Figure 1A, C, E, and G), BALF macrophages were increased following instillation of AgNPs but the temporal pattern of this increase, as well as the percentage of BALF macrophages containing silver (Figure 1B, D, F, and H) varied with particle size and coating. The smaller 20 nm AgNPs were more effective at increasing macrophage numbers at either 1 or 7 d following exposure than the 110 nm particles. Only the 20 nm citrate AgNP resulted in statistically significant increases in macrophage numbers in lavage that persisted to 21 d post exposure (Figure 1A) as all other groups returned to control values by 21 d (Figure 1C, E, and G). Only the 110 nm citrate AgNP was not able to induce an acute increase in macrophage cell numbers at 1 d post exposure (Figure 1C). By 24 h, the percentage of macrophages that were positive for silver varied from a high of 38% in the 110 nm PVP group to a low of 22% in the 110 nm

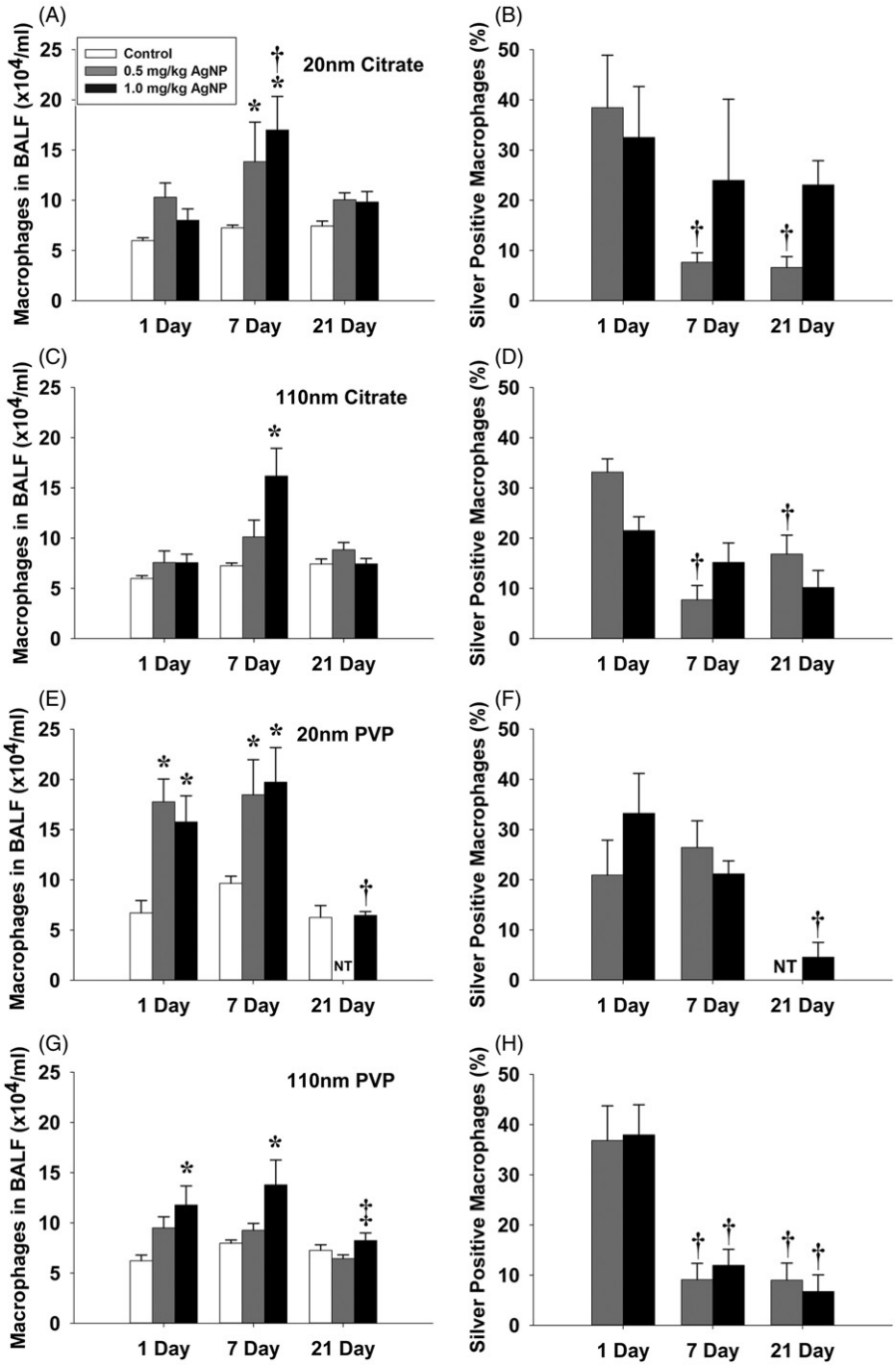

Figure 1. Total macrophages (A, C, E, and G) and percentage of silver positive macrophages (B, D, F, and H). In BALF 1, 7, or 21 d, after i.t. instillation of four types of silver nanoparticles of two doses (0.5 and 1.0 mg/kg). (A and B) 20 nm citrate, (C and D) 110 nm citrate, (E and F) 20 nm PVP, and (G and H) 110 nm PVP. *Significantly greater than control at same timepoint ($p < 0.05$). †Significantly different from same dose at 1 d timepoint ($p < 0.05$) ($n = 6$). NT, not tested.

citrate group, but all particle exposures resulted in the detection of silver positive macrophages (Figure 1B, D, F, and H). Instillation of 1.0 mg/kg of the 20 nm citrate-coated AgNP produced the greatest percentage of silver positive macrophages persisting to 21 d post exposure (Figure 1B). Interestingly, this was significantly greater than in the group exposed to the same size particles but with a PVP coating (Figure 1F). There was no difference in the percentage of positive macrophages with increasing dose except for the 20 nm citrate AgNP at 21 d ($p = 0.049$), where the 1.0 mg/kg dose was significantly higher than the 0.5 mg dose at that timepoint (Figure 1B).

To assess the differences in internalized silver in the macrophage population, we created a silver uptake score (Figure 2). This system gives greater weight to macrophages staining heavily for silver resulting in higher scores in treatment groups with a high percentage of heavily stained macrophages. This more clearly delineates that the 20 nm citrate-coated particles have the greatest degree of macrophage involvement 21 d post exposure (Figure 2A). Additionally, uptake of AgNPs was demonstrated in TEM micrographs of macrophages containing particles (Figure 3). A 110-nm AgNP is located in a vacuole in Figure 3(A) and (B) (open arrow). Figure 3(C) shows a different macrophage with a silver particle in a lysosome.

Localization of silver in lung tissue

The abundance of silver and distribution of AgNPs was determined in lung tissue using ICP-MS on the right middle lung lobe and autometallography on tissue sections from the left lung lobe of the same animals. Surface coating of the AgNPs had the largest effect on silver clearance from the tissue with PVP-coated AgNPs showing significant clearance of 20 nm AgNP ($p = 0.013$) and 110 nm AgNP nearly significant ($p = 0.078$) at 21 d after exposure (Figure 4). There was no difference in particle

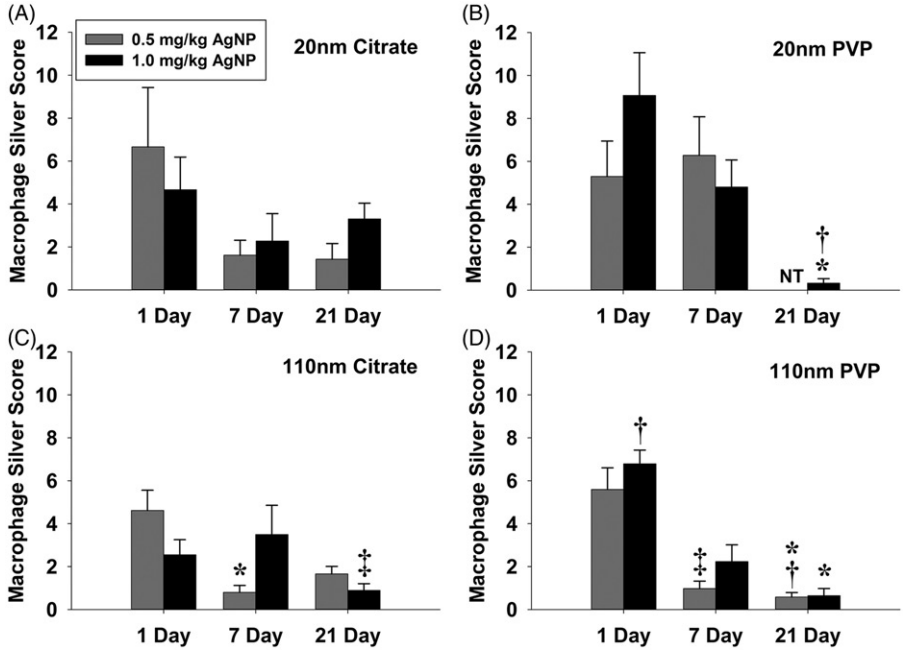

Figure 2. BALF macrophage silver uptake scores. Macrophages were scored based on the intensity of silver staining (light, moderate, or heavy) as shown in Figure S1 and adjusted for the total number of silver positive macrophages that were recovered from BALF to generate a macrophage silver uptake score for each treatment group and timepoint. *Significantly different than 1 d timepoint for same AgNP size, coating, and dose; †significantly different between citrate- and PVP-coated AgNP at same timepoint, AgNP size, and dose; ‡Significantly different between 20 nm and 110 nm AgNP at same timepoint, AgNP coating, and dose ($p < 0.05$) ($n = 5$–6).

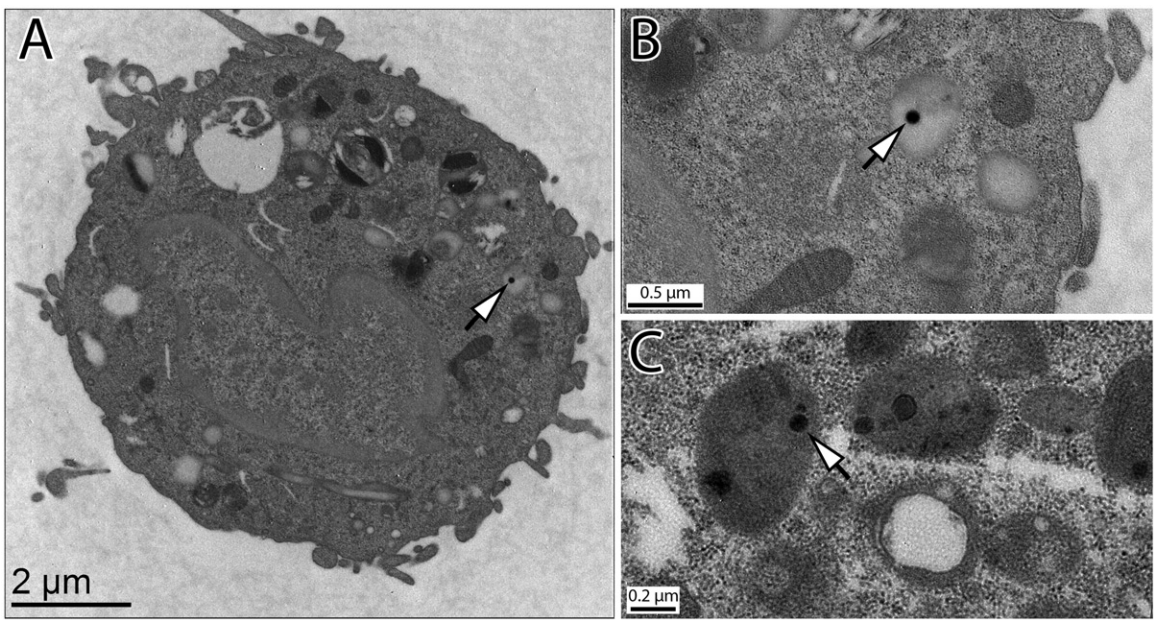

Figure 3. TEM image of macrophages containing silver particles. An (A) overview and (B) detail of an AgNP (open arrow) in a vacuole of a macrophage recovered from BALF. (C) An example of an AgNP (open arrow) in the lysosome of a BALF-recovered macrophage.

clearance by particle size. Interestingly, there was a lack of significant clearance of both citrate-coated AgNPs even at 21 d after a single acute exposure, although there was quite a bit of variance in these measurements with a range from 0 to 1.6 µg/g in the 20 nm citrate and a range of 0 to 2.8 µg/g in the 110 nm citrate. The following decreases in measured silver were observed at 21 d when compared with lobes containing particles of the same size 1 d after instillation: 2% for the 20 nm citrate, 91% for the 20 nm PVP, 9% for the 110 nm citrate, and 71% for the 110 nm PVP.

Examination of the intrapulmonary lobar bronchus of the left lobe indicated that at 1 d post exposure, the 110 nm AgNP was removed from the larger airways more completely than the 20 nm AgNP (compare Figure 5B and D with Figure 5A and C). The silver was heavily localized to the surface epithelium and was found on the cilia as well as within Clara cells and this intracellular localization was especially prominent for the citrate-coated AgNPs (Figure 5A). At the same time point (1 d post exposure), silver was intensely localized to the most distal-conducting airways, the terminal bronchioles, and the immediately adjacent bronchoalveolar regions in all groups (Figure 6A, C, E, and G). Silver was localized to the surface epithelial cells including dark intracellular staining in Clara cells (Figure 6B, D, F, and H) and was also found in the subepithelial basement membrane zone. Subepithelial localization to the basement membrane zone was especially prominent in the 20 nm citrate and 20 nm PVP groups (Figure 6B and F). All groups had intense staining of tissue macrophages associated with the basement membrane zone; however, the silver staining was less abundant

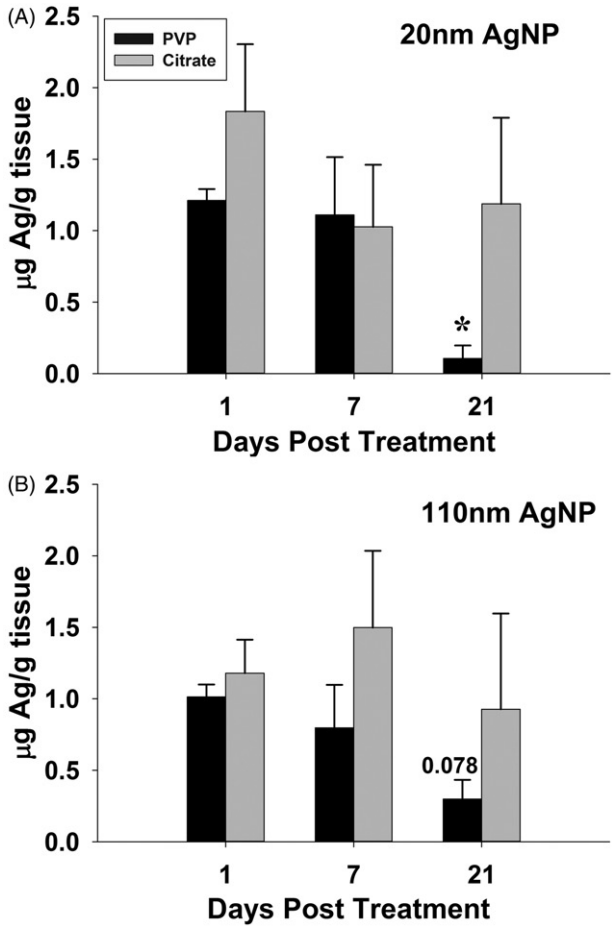

Figure 4. Silver quantification in the right middle lung lobe by ICP-MS following 1.0 mg/kg dose of AgNPs. (A) 20 nm AgNPs-treated animals and (B) is 110 nm AgNPs-treated animals. Black bars are PVP-coated AgNPs and grey bars are citrate-coated AgNPs. *Significantly different than 1 d time-point for the same AgNP size and coating ($p < 0.05$) ($n = 6$).

for the larger 110 nm AgNPs (Figure 6C and G) compared with the 20 nm AgNPs (Figure 6A and E).

At 7 d post exposure (Figure 7A–H), silver was heavily localized to the basement membrane zone of the terminal bronchioles, alveolar macrophages, and immediately adjacent alveoli of the bronchoalveolar duct junction. This was the only region of the lung that contained heavy staining at this timepoint; the larger airways and more peripheral alveoli did not contain detectable silver (Figure S3). Silver was also localized to the vascular endothelium in this region (Figure 8F). In contrast to 1 d post exposure, the epithelium of the most distal portion of the terminal bronchiole no longer contained large accumulations of silver (compare Figure 6 with Figure 7). This staining pattern was similar between AgNPs of different sizes and surface coatings. However, some cells in the more proximal portion of the terminal bronchiole contained silver accumulations in the epithelium and this included both cytoplasmic and nuclear staining of Clara and ciliated cells (Figure S4). Frank epithelial cytotoxicity was not seen in the high-resolution histopathology for any timepoint or type of AgNPs (data not shown). At 21 d post exposure (Figure S5), silver was still detectable in focal areas of some of the terminal bronchioles. The few areas of the terminal bronchiole/alveolar duct region that did have localized staining at this timepoint are shown in Figure S5. There was no difference in the abundance of these regions by particle type. Silver was also found in tissue macrophages but was greatly diminished in all groups compared with the pattern at 1 and 7 d. To give an assessment of the range of staining within the tissue, we used a semiquantitative scoring method to illustrate overall tissue terminal bronchiole/alveolar duct junction staining intensity by days after exposure (Figure 8). This illustrates the significant reduction in silver localization in this lung region by 21 d after exposure in all the exposure groups.

Discussion

We tested AgNPs of two sizes (110 versus 20 nm) and two surface coatings (citrate versus PVP) at two doses (0.5 and 1.0 mg/kg) in adult male rats. Our results show that AgNPs and/or silver in some form persists in the lungs as long as 21 d following a single acute i.t. exposure. Further, the particle size has a modest effect on the amount retained in the lung tissue but particle coating heavily influences the retention of silver in the lung at 21 d. The PVP-coated material cleared more quickly than the citrate-coated material. Macrophages were heavily involved in clearance of the material, especially the 20 nm citrate-coated material, even at 21 d following a single acute exposure.

There is debate about the constituents or chemical state of AgNP that contributes to their health effects (Behra et al., 2013). It is not clear whether it is the silver ions released from the AgNP (Wang et al., 2014), or the AgNP themselves, that cause adverse health effects (Beer et al., 2012; Cronholm et al., 2013; Gliga et al., 2014). Our study was not designed to define whether the silver in the lung was ionic, but rather to probe whether the AgNP we added to the lungs of rats persisted in the lung, as any form of silver, over time. Recent work using the same AgNPs (Wang et al., 2014) found that 20 nm particles, regardless of coating, shed a greater amount (~4%) of silver ion into BEGM medium *in vitro* than larger particles. We note that measurement of release of silver ions from nanomaterials into tissues *in vivo* has not been accomplished to date and may have different kinetics than *in vitro* systems. Some inference may be made from other studies of silver nanoparticles and soluble silver ions. In a study in rats, instilled ionic silver ($AgNO_3$) was found to be rapidly cleared in contrast to instilled ultrafine silver particles with only 25% of the day one ionic lung dose remaining in the lung at 7 d (Takenaka et al., 2001). Silver ion binding to proteins was thought to be a potential mechanism for the retention of ions as long as 7 d. A study by Wang et al. used the same particles as in the current study and found that significant less $AgNO_3$ was retained 40 h after exposure than either the 20 nm or 110 nm AgNP (Wang et al., 2014) and that $AgNO_3$-administered silver was undetectable in the mouse lung 21 d after exposure, in contrast to significant persistence of AgNP silver as measured by ICP-MS. In this study, we performed autometallography on lung samples 1 d post treatment with $AgNO_3$ (see Supplementary materials). At 1 d post exposure, the pattern of staining in the $AgNO_3$ differed considerably, with very diffuse and spotty staining (Figure S6). The autometallographic and ICP-MS methods we used do not discriminate between ionic and particle bound silver. Autometallography is most likely to detect areas of heavy silver localization and less likely to detect diffuse accumulations throughout the tissue. Further, the staining protocol was optimized to detect staining at 1-d post exposure and the same development practices were used for all the timepoints in this study to facilitate comparisons. This may be why the autometallography detects little silver at 21 d post exposure but the ICP-MS measurement indicates that significant silver persists in the lung at this timepoint. If the smaller particles have higher dissolution rates *in vivo*, as has been demonstrated *in vitro* (Wang et al., 2014), this could be related to the observed increased deposition of silver in the subepithelial basement membrane zone that was noted for the 20 nm particles at 1 d after exposure (Figure 7).

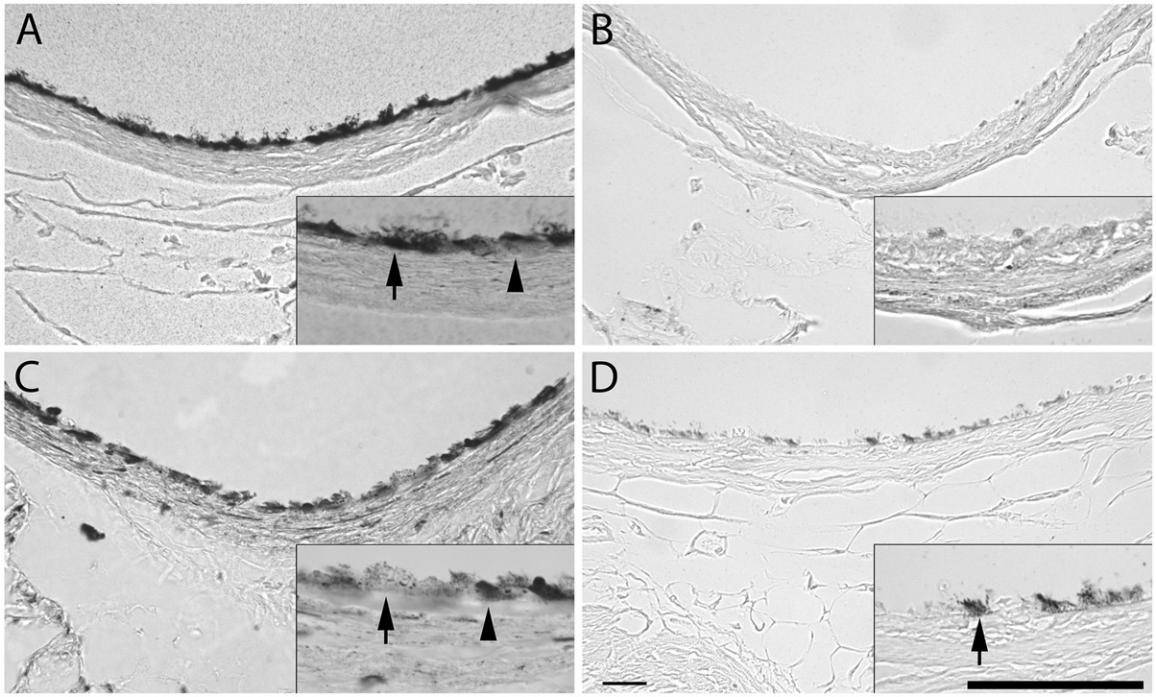

Figure 5. Autometallography (dark staining) of silver localization on and within the epithelium of the proximal airways (intrapulmonary lobar bronchus) 1 d post exposure to 1.0 mg/kg AgNPs. (A) 20 nm citrate, (B) 110 nm citrate, (C) 20 nm PVP, and (D) 110 nm PVP. Note the staining on the ciliated cell (arrows) as well as within Clara cells (arrowheads). Bars = 50 μm.

Macrophages play a critical role in particle clearance in the lung. A study of 25 nm inhaled titanium dioxide found that macrophages had sporadic uptake of particles at 24 h after exposure (Geiser et al., 2008), indicating that phagocytosis of nanometer-sized particles is fairly inefficient (Geiser, 2010). Other studies have indicated that smaller magnetite (Fe_3O_4) nanoparticles (10 nm) are less potent at inducing macrophage influx into the lung larger than 50 nm particles (Katsnelson, 2010). In addition, studies of gold nanoparticles of three sizes (2, 40, and 100 nm) given by intratracheal instillation found that lung macrophages have very rapid uptake of particles with instilled nanoparticles already localized to macrophages 1 h after a single instillation and localized to macrophage lysosome-like vesicles (Sadauskas et al., 2009). Other studies of intratracheally instilled silver have also noted macrophage accumulation of silver nanoparticles in phagolysosomes of alveolar macrophages (Takenaka et al., 2001). Our data indicate similar findings; macrophages are involved in scavenging silver or silver NP at all timepoints examined and the intracellular localization of the silver was to lysosome-like vesicles. In general, the smaller silver particles induced a greater maximal measured macrophage influx than the larger ones. This may be related to the composition or the number of particles. A dose of 1.0 mg/kg instilled in the average weight rat from this study (359.5 g) would be equal to 1.45×10^{16} particles/rat for the 20 nm AgNP and 8.74×10^{13} particles/rat for the 110 nm AgNP. The number of 20 nm particles instilled in rats is 166 times greater than the 110 nm particles. While the particle size did not influence macrophage influx into BALF at 1 d post exposure, the 1 mg/kg dose 110 PVP AgNP macrophage silver score was significantly higher than the 110 nm citrate AgNP indicating a difference by particle coating. We found that the 20 nm citrate particles had the highest macrophage silver score at 21 d after exposure. This may be due to a higher number of smaller particles being present in the sub-alveolar regions, greater bioavailability of these particles or differences in particle shedding of ions.

Particles that deposit in the large airway are removed through the mucociliary escalator and this is still occurring at 1 d but is diminished at 7 d post exposure (Figure S3). This mechanism is an effective early response for removal of the larger particles. One study using insoluble particles of 0.1, 1, 2, and 7 μm found that the mucociliary clearance halftime for rats is 1.25 h (Hofmann & Asgharian, 2003). In contrast, a study using 15 nm iridium (Ir) particles found 18% clearance into the gastrointestinal tract after 6 h (Kreyling et al., 2002). This suggests that clearance of smaller nanoparticles is slower. However, a recent study by Kreyling et al. found that there was a large variability in mucociliary-cleared AuNP fraction at 24 h between animals ($n = 4$) for particles of different sizes with the largest variance noted for particles that were 1.4 nm (Kreyling et al., 2014). However, the variance for the larger particles was less and is in good agreement with our current data ($n = 6$). Our current study shows that persistence of the smaller (20 nm) silver particles in the lung is in agreement with other studies that show that smaller particles are more efficiently translocated to interstitial spaces and are slower to clear (Kreyling et al., 2002). Thus, while macrophage numbers are increased in response to all four particle types, there is a different temporal pattern by particle type with the smaller particles inducing an early increase in BALF macrophages at the lower 0.5 mg/kg dose at 1 d post exposure, possibly due to their larger surface area. However, we note that due to the 6 d period between our first two sampling points we cannot rule out that other exposure groups may have had a peak macrophage influx that we did not detect.

Macrophages have a substantial role in scavenging the silver present in the distal lung even 21 d following the initial particle exposure. This is evident from the detectable levels of silver-containing macrophages in the BALF of all exposure groups. However, only one of the particle types tested, the 20 nm citrate-coated AgNP, still induced a significant increase in BALF macrophages at 21 d after exposure. Notably this was also the exposure group with the highest percentage of silver positive

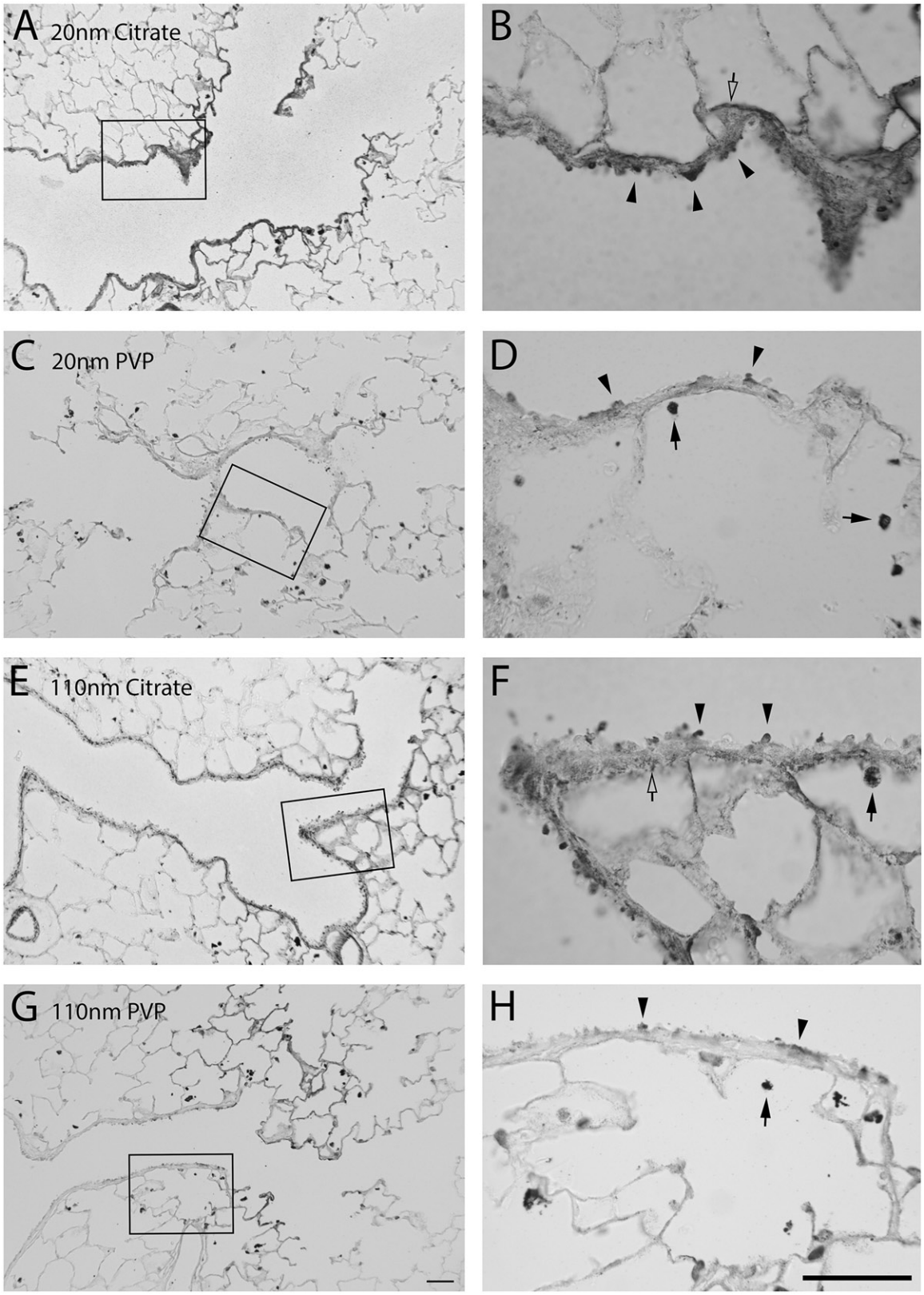

Figure 6. Autometallography (dark staining) of silver localization in the terminal bronchiole alveolar duct junction at 1 d post exposure to 1.0 mg/kg AgNPs. (A and B) 20 nm citrate, (C and D) 110 nm citrate, (E and F) 20 nm PVP, and (G and H) 110 nm PVP. Clara cells (arrowheads) and macrophages (arrows) as well as the subepithelial basement membrane zone (open arrows) contained silver. Bars = 50 μm.

macrophages at 21 d. Interestingly, there were no large differences in total macrophage numbers or numbers of positive macrophages by dose, with the exception of the 20 nm citrate AgNP at 21 d post exposure, possibly indicating a maximum for macrophage-mediated removal at these two doses in the lung.

Our study found that instilled AgNPs result in silver accumulation in the lung tissue itself both within the epithelium acutely and within macrophages and in the subepithelial basement membrane zone. The accumulation at 1 d followed by clearance of the silver from Clara cells at 7 d may indicate an active role for

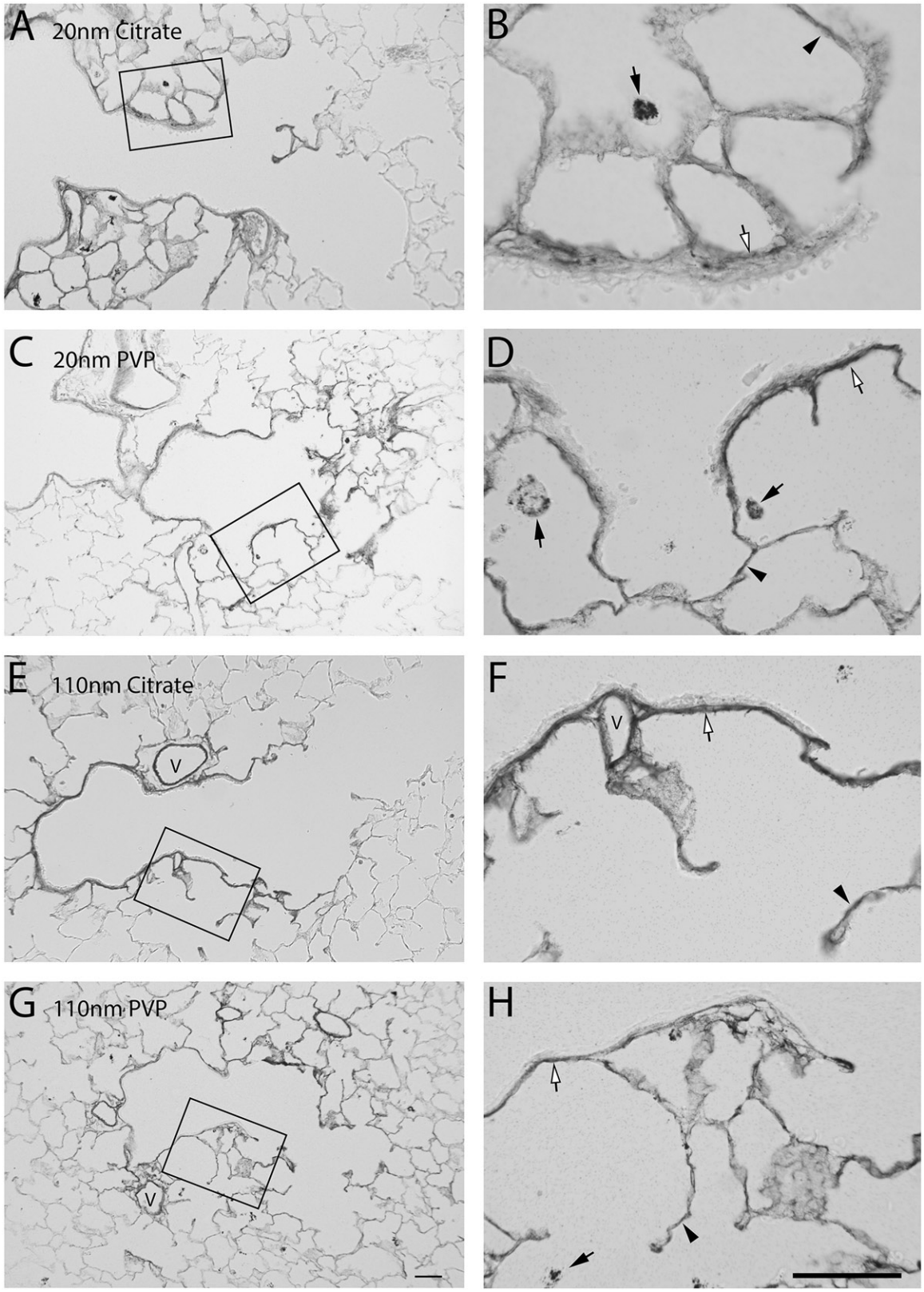

Figure 7. Autometallography (dark staining) of silver localization to the terminal bronchiole alveolar duct junction at 7 d post exposure to 1.0 mg/kg AgNPs. (A and B) 20 nm citrate, (C and D) 110 nm citrate, (E and F) 20 nm PVP, and (G and H) 110 nm PVP. Macrophages (arrows), basement membrane zone (open arrows), alveolar walls (arrowheads), and vessels (V) contained heavy localization of silver. Clara cells were not stained. Bars = 50 μm.

Clara cells in nanoparticle processing. Clara cells have previously been reported to endocytose surfactant protein D into secretory granules located at the apex of the cell (Voorhout et al., 1992). Our findings are in agreement with *in vitro* studies of other lung epithelial cells (BEAS-2B) that showed accumulation of AgNPs over 24 h (Gliga et al., 2014; Wang et al., 2014) and preferential accumulation of AgNPs versus a soluble silver salt *in vitro* (Cronholm et al., 2013; Wang et al., 2014). This raises several

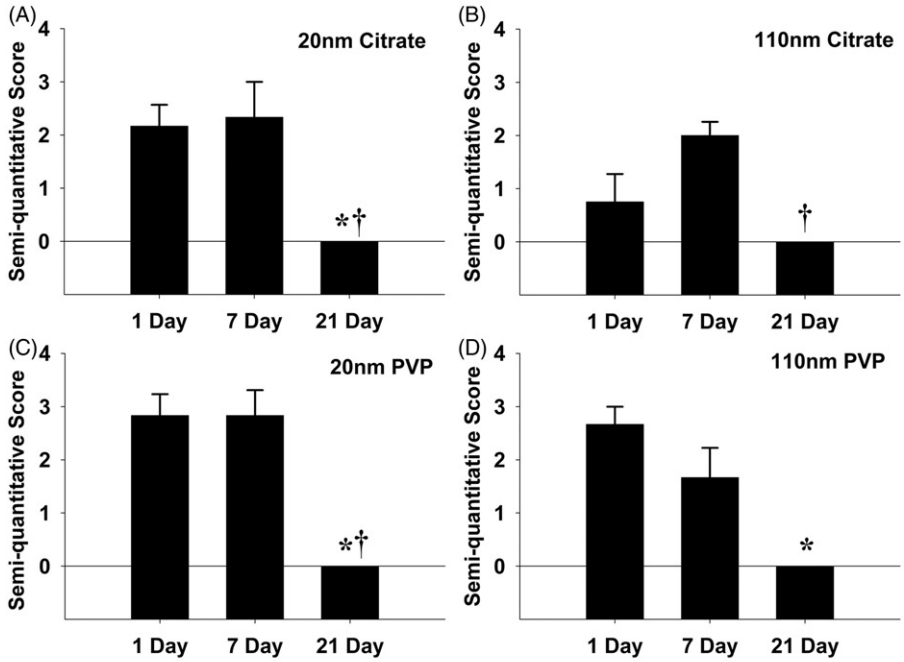

Figure 8. Semi-quantitative scoring of silver distribution in the terminal bronchiole region. (A) 20 nm citrate, (B) 110 nm citrate, (C) 20 nm PVP, and (D) 11 0 nm PVP. *Significantly less than 1 d post treatment ($p < 0.05$); †significantly less than 7 d post treatment ($p < 0.05$) ($n = 6$).

interesting questions, including: why does the silver accumulate in the subepithelial basement membrane zone at 7 d post exposure and is it still confined to AgNPs at this time? There are several possibilities: the epithelial cells could secrete the particles or the silver ions basolaterally, the components of the basement membrane zone could preferentially sequester the silver or the particles, or possibly the AgNP distribution is fairly uniform throughout the lung initially but the basement membrane zone is a difficult area to clear of nanosilver or its ions. A similar staining pattern was found in the parallel mouse studies and correlated with the expression of basement membrane collagen (Wang et al., 2014). In contrast to Wang et al., the subepithelial silver staining in the current rat study resolved by 21-d post exposure. This may indicate the removal by macrophages or turnover of the molecules binding silver. Other studies report silver sequestration to subepithelial basement membranes in the skin following silver dietary supplement intake (Bowden et al., 2011). A study of silver ion release from implanted silver surfaces noted accumulation of silver in lysosome-like organelles and associated with collagen fibers in the basement membrane of multiple organs (Danscher & Stoltenberg, 2010). It remains to be determined which molecules preferentially bind either AgNP or Ag ions in the basement membrane zone of the lung and the precise subcellular localization of the silver.

The doses used in this study are comparable with a similar study using the same particles in mice (Wang et al., 2014). These doses were selected to model an environmental exposure (5–289 μg/m^3) that occurred in a manufacturing facility (Lee et al., 2012) and to facilitate cross species comparisons. In Wang et al., both sizes of the citrate-coated AgNPs cleared similarly (approximately 60%) over the period of 2–21 d post a single acute exposure in mice. Our measured clearance rate for the same particles between 1 and 21 d post exposure in rats was clearly less (25–50%) and also did not show a significant decrease with time post exposure, indicating a possible species difference in response for the citrate-coated particles. This may be partially due to the fact that the right middle lung lobe was lavaged before freezing and so our measurements of silver retention only account for that which was still incorporated in the tissue itself. However, the fraction of lavagable particles is likely to be small, as demonstrated in a study of 20 nm ^{192}Ir particles that found only 14% of the particles were in the lavage 24 h after exposure (Semmler-Behnke et al., 2007). This supports the thought that particles rapidly associate with lung tissue. Interestingly, our measured PVP clearance data found greater than 75% clearance between 1 and 21 d post exposure, on par with the data reported by Wang et al. for citrate particles in mice (they did not report PVP clearance). Clearly there is preferential clearance of PVP-coated particles compared with citrate-coated particles in our rat model. Further, we can relate our clearance from the lung tissue for all four particle types in terms of the percentage of the initial delivered dose of each particle size with 2% and 91% clearance of 20 nm citrate and PVP AgNPs, respectively, and 9% and 71% for citrate and PVP 110 nm AgNPs, respectively. Previous studies of fluorescent 20 nm and 100 nm polystyrene spheres found that the 20 nm spheres have a greater propensity to stay in the body (Sarlo et al., 2009). A study of aerosolized and instilled ultrafine ^{192}Ir particles at either 15 or 80 nm in rats showed that most particles stayed in the lung at 7 d (Kreyling et al., 2002) in agreement with our current study.

It is important to keep in mind that while useful for directly comparing doses of compound and screening large numbers of compounds quickly, instillation exposure of AgNP in liquid has limitations in regard to health assessment of possible environmental exposure to an aerosol of dry or aqueous material. The retention pattern could be different because deposition pattern is different; other studies show that clearance of instilled particles is slower than that of comparable particles that are inhaled (Driscoll et al., 2000). Whether retention of inhaled AgNP is similar needs to be determined in future studies of inhaled particles of the same type. Instillation can result in a non-uniform distribution between lung lobes. Our staining studies using autometallography for the left lung lobe support a uniform distribution of the silver within the lobe with consistent deposition in similar regions, including bronchiolar alveolar duct junctions, throughout the lung regardless of the particle type. However, the distribution to other lobes, especially those such as the right middle lung lobe, which we used for the ICP-MS measurements, may be less uniform. This is

supported by the amount of variance in the ICP-MS data from this lobe (Figure 4). We note that, even with the measured variance, there was sufficient power to detect a decrease in the silver content of the lung for the PVP-coated particles at 21 d post exposure.

Conclusion

In conclusion, our study shows that silver associated with PVP-coated particles is most efficiently cleared from the lung at 21 d following acute exposure and that the 20 nm citrate-coated AgNP result in the greatest amount of silver still present in the lungs at 21 d. In general, persistence of silver in the lung correlated with increased BALF macrophages and higher percentages of silver positive BALF macrophages. As early as 1 d following exposure, differences in particle removal were apparent with the 110 nm particles more efficiently removed from the larger airways. The current study supports a large effect of particle surface coating on both persistence and biological effect (macrophage recruitment and involvement), with a lesser effect of particle size.

Acknowledgements

We are grateful to the following people for their skilled technical assistance during sample collection and processing: Ryan Mendoza, Imelda Espiritu, and Janice Peake. Imaging was conducted at the UC Davis Cellular and Molecular Imaging core. We thank the UC Davis Interdisciplinary Center for Inductively-Coupled Plasma Mass Spectrometry and both Peter Green and Joel Commisso for assistance with the ICP-MS samples and analysis. We thank the UC Davis Electron Microscopy Laboratory, Department of Medical Pathology and Laboratory Medicine, School of Medicine and Patricia Kysar for assistance with the macrophage TEM images.

Declaration of interest

The authors declare that they have no competing interests. Grant support (U01 ES020127) and silver nanomaterials used in this study are procured, characterized, and provided to investigators by the NIEHS Centers for Nanotechnology Health Implications Research (NCNHIR) Consortium. We acknowledge a Superfund Research Program Fellowship in support of Donald Anderson (P42 ES004699) and the Western Center for Agricultural Health and Safety (NIOSH Grant 0H07550) for Rona Silva. The NIEHS Centers for Nanotechnology Health Implications Research (NCNHIR) was established with the centers funded by RFA ES-09-011. These centers formed a consortium with other NIEHS funded researchers in the area of Nano EHS and worked together on a select set of engineered nanomaterials provided to the consortium by NIEHS. Any opinions, findings, conclusions, or recommendations expressed herein are those of the author(s) and do not necessarily reflect the views of the National Institute of Environmental Health Sciences or NIH.

References

Abid AD, Anderson DS, Das GK, Van Winkle LS, Kennedy IM. 2013. Novel lanthanide-labeled metal oxide nanoparticles improve the measurement of in vivo clearance and translocation. Part Fibre Toxicol 10:1.

Adachi A, Fukunaga A, Hayashi K, Kunisada M, Horikawa T. 2003. Anaphylaxis to polyvinylpyrrolidone after vaginal application of povidone–iodine. Contact Dermat 48:133–6.

Baisch BL, Corson NM, Wade-Mercer P, Gelein R, Kennell AJ, Oberdorster G, Elder A. 2014. Equivalent titanium dioxide nanoparticle deposition by intratracheal instillation and whole body inhalation: the effect of dose rate on acute respiratory tract inflammation. Part Fibre Toxicol 11:5.

Beer C, Foldbjerg R, Hayashi Y, Sutherland DS, Autrup H. 2012. Toxicity of silver nanoparticles – nanoparticle or silver ion? Toxicol Lett 208: 286–92.

Behra R, Sigg L, Clift MJ, Herzog F, Minghetti M, Johnston B, et al. 2013. Bioavailability of silver nanoparticles and ions: from a chemical and biochemical perspective. J R Soc Interface 10:20130396.

Bowden LP, Royer MC, Hallman JR, Lewin-Smith M, Lupton GP. 2011. Rapid onset of argyria induced by a silver-containing dietary supplement. J Cutan Pathol 38:832–5.

Coppens JT, Van Winkle LS, Pinkerton K, Plopper CG. 2007. Distribution of Clara cell secretory protein expression in the tracheobronchial airways of rhesus monkeys. Am J Physiol Lung Cell Mol Physiol 292:L1155–62.

Cronholm P, Karlsson HL, Hedberg J, Lowe TA, Winnberg L, Elihn K, et al. 2013. Intracellular uptake and toxicity of Ag and CuO nanoparticles: a comparison between nanoparticles and their corresponding metal ions. Small 9:970–82.

Danscher G, Locht LJ. 2010. In vivo liberation of silver ions from metallic silver surfaces. Histochem Cell Biol 133:359–66.

Danscher G, Stoltenberg M. 2006. Silver enhancement of quantum dots resulting from (1) metabolism of toxic metals in animals and humans, (2) *in vivo*, *in vitro* and immersion created zinc–sulphur/zinc–selenium nanocrystals, (3) metal ions liberated from metal implants and particles. Prog Histochem Cytochem 41:57–139.

Driscoll KE, Costa DL, Hatch G, Henderson R, Oberdorster G, Salem H, Schlesinger RB. 2000. Intratracheal instillation as an exposure technique for the evaluation of respiratory tract toxicity: uses and limitations. Toxicol Sci 55:24–35.

Fabrega J, Luoma SN, Tyler CR, Galloway TS, Lead JR. 2011. Silver nanoparticles: behaviour and effects in the aquatic environment. Environ Int 37:517–31.

Geiser M. 2010. Update on macrophage clearance of inhaled micro- and nanoparticles. J Aerosol Med Pulm Drug Deliv 23:207–17.

Geiser M, Casaulta M, Kupferschmid B, Schulz H, Semmler-Behnke M, Kreyling W. 2008. The role of macrophages in the clearance of inhaled ultrafine titanium dioxide particles. Am J Respir Cell Mol Biol 38: 371–6.

Gliga AR, Skoglund S, Wallinder IO, Fadeel B, Karlsson HL. 2014. Size-dependent cytotoxicity of silver nanoparticles in human lung cells: the role of cellular uptake, agglomeration and Ag release. Part Fibre Toxicol 11:11.

Hacker GW, Grimelius L, Danscher G, Bernatzky G, Muss W, Adam H, Thurner J. 1988. Silver acetate autometallography – an alternative enhancement technique for immunogold-silver staining (Igss) and silver amplification of gold, silver, mercury and zinc in tissues. J Histotechnol 11:213–21.

Hofmann W, Asgharian B. 2003. The effect of lung structure on mucociliary clearance and particle retention in human and rat lungs. Toxicol Sci 73:448–56.

Huynh KA, Chen KL. 2011. Aggregation kinetics of citrate and polyvinylpyrrolidone coated silver nanoparticles in monovalent and divalent electrolyte solutions. Environ Sci Technol 45:5564–71.

Katsnelson B, Privalova LI, Kuzmin SV, Degtyareva TD, Sutunkova MP, Yeremenko OS, et al. 2010. Some peculiarities of pulmonary clearance mechanisms in rats after intratracheal instillation of magnetite (Fe_3O_4) suspensions with different particle sizes in the nanometer and micrometer ranges: are we defenseless against nanoparticles? Int J Occup Environ Health 16:508–24.

Kreyling WG, Hirn S, Moller W, Schleh C, Wenk A, Celik G, et al. 2014. Air-blood barrier translocation of tracheally instilled gold nanoparticles inversely depends on particle size. ACS Nano 8:222–33.

Kreyling WG, Semmler M, Erbe F, Mayer P, Takenaka S, Schulz H, et al. 2002. Translocation of ultrafine insoluble iridium particles from lung epithelium to extrapulmonary organs is size dependent but very low. J Toxicol Environ Health A 65:1513–30.

Lee J, Ahn K, Kim S, Jeon K, Lee J, Yu I. 2012. Continuous 3-day exposure assessment of workplace manufacturing silver nanoparticles. J Nanopart Res 14:1134.

Pelgrift RY, Friedman AJ. 2013. Nanotechnology as a therapeutic tool to combat microbial resistance. Adv Drug Deliv Rev 65:1803–15.

Pritchard JN, Holmes A, Evans JC, Evans N, Evans RJ, Morgan A. 1985. The distribution of dust in the rat lung following administration by inhalation and by single intratracheal instillation. Environ Res 36: 268–97.

Quadros ME, Marr LC. 2010. Environmental and human health risks of aerosolized silver nanoparticles. J Air Waste Manag Assoc 60:770–81.

Rönnau AC, Wulferink M, Gleichmann E, Unver E, Ruzicka T, Krutmann J, Grewe M. 2000. Anaphylaxis to polyvinylpyrrolidone in an analgesic preparation. Br J Dermatol 143:1055–8.

Sadauskas E, Jacobsen N, Danscher G, Stoltenberg M, Vogel U, Larsen A, et al. 2009. Biodistribution of gold nanoparticles in mouse lung following intratracheal instillation. Chem Cent J 3:16.

Sarlo K, Blackburn KL, Clark ED, Grothaus J, Chaney J, Neu S, et al. 2009. Tissue distribution of 20 nm, 100 nm and 1000 nm fluorescent polystyrene latex nanospheres following acute systemic or acute and repeat airway exposure in the rat. Toxicology 263:117–26.

Seltenrich N. 2013. Nanosilver: weighing the risks and benefits. Environ Health Perspect 121:a220–5.

Semmler-Behnke M, Takenaka S, Fertsch S, Wenk A, Seitz J, Mayer P, et al. 2007. Efficient elimination of inhaled nanoparticles from the alveolar region: evidence for interstitial uptake and subsequent reentrainment onto airways epithelium. Environ Health Perspect 115: 728–33.

Smith DR, Fickett FR. 1995. Low-temperature properties of silver. J Res or Natl Inst Stand Technol 100:119–71.

Takenaka S, Karg E, Roth C, Schulz H, Ziesenis A, Heinzmann U, et al. 2001. Pulmonary and systemic distribution of inhaled ultrafine silver particles in rats. Environ Health Perspect 109 Suppl 4:547–51.

Van Winkle LS, Buckpitt AR, Nishio SJ, Isaac JM, Plopper CG. 1995. Cellular response in naphthalene-induced Clara cell injury and bronchiolar epithelial repair in mice. Am J Physiol 269: L800–18.

Voorhout WF, Veenendaal T, Kuroki Y, Ogasawara Y, Van Golde LM, Geuze HJ. 1992. Immunocytochemical localization of surfactant protein D (SP-D) in type II cells, Clara cells, and alveolar macrophages of rat lung. J Histochem Cytochem 40:1589–97.

Wang X, Ji Z, Chang CH, Zhang H, Wang M, Liao YP, et al. 2014. Use of coated silver nanoparticles to understand the relationship of particle dissolution and bioavailability to cell and lung toxicological potential. Small 10:385–98.

Yoshida K, Sakurai Y, Kawahara S, Takeda T, Ishikawa T, Murakami T, Yoshioka A. 2008. Anaphylaxis to polyvinylpyrrolidone in povidone-iodine for impetigo contagiosum in a boy with atopic dermatitis. Int Arch Allergy Immunol 146:169–73.

Supplementary material available online
Supplementary Figures S1–S6 and Table 1